Studies in Surface Science and Catalysis 144
F. Rodríguez-Reinoso, B. McEnaney, J. Rouquerol and K. Unger (Editors)

Structural studies of mesoporous alumina membranes by small angle X-ray scattering

John C. Dore[a], Robert E. Benfield[a], Didier Grandjean[a], Günter Schmid[b], Michael Kröll[b,d] and David Le Bolloc'h[c,e]

[a]Centre for Materials Research, School of Physical Sciences, University of Kent, Canterbury CT2 7NR, U.K.
[b]Institut für Anorganische Chemie, Universität GH Essen, Universitätsstr. 5-7, D-45117 Essen, Germany.
[c]European Synchrotron Radiation Facility, 38043 Grenoble Cedex, France.
[d]present address: Physics Department, Trinity College Dublin, Dublin 2, Ireland.
[e]present address: Laboratoire de Physique des Solides, Bât. 510, Univ. Paris Sud, 91405 Orsay, France.

Small-angle X-ray scattering (SAXS) has been used to study the structures of mesoporous alumina membranes. These membranes, produced by anodic deposition, have an arrangement of parallel cylindrical pores centred on a disordered hexagonal lattice. The SAXS intensity profile varies over five orders of magnitude, and is a convolution of a structure factor for the 2D distribution of pore axes with a cylinder form factor for the pores. Rotation of the plane of the membrane changes the pattern from a ring structure for channels parallel to the X-ray beam to a set of vertical spots for channels perpendicular to the beam. The oscillatory pattern changes systematically with the anodic deposition voltage, confirming a linear relationship between voltage and pore separation. Initial results are also reported for alumina membranes containing cobalt nanowires in the pore volume. The SAXS technique complements and extends direct-imaging methods such as electron microscopy, which view only the surface structure for a limited area of the sample. The results indicate that the membranes show greater disorder than normally deduced from other techniques.

1. INTRODUCTION

Mesoporous alumina membranes ("anodic aluminium oxide", or AAO) are prepared by anodic oxidation of aluminium metal [1,2]. The cylindrical pores, perpendicular to the membrane surface, form hexagonal arrays of straight non-intersecting channels with pore densities up to $10^{11}/cm^2$. Their diameters are controllable within the range 5 – 100 nm as a linear function of anodisation voltage. These membranes are used as molecular sieves, and have also found application as templates for metallic nanowires [3,4,5,6], metal clusters and colloids [7,8], and carbon nanotubes [9,10].

Structural characterisation of AAO membranes has been based mainly on direct imaging methods such as scanning or transmission electron microscopy [3,4,11]. These techniques image only a small area or volume of the material, which may not be representative of the overall structure or long-range order. To understand and control the properties of these membranes as host materials, a more complete structural characterisation is required.

Although small-angle X-ray scattering (SAXS) has been widely used to study porous solids, there have been few previous applications to membranes containing regular arrays of parallel pores. A preliminary USAXS (ultra-small angle X-ray scattering) study of AAO membranes has given a measurement of inter-pore distance [12]. A small-angle neutron scattering (SANS) study placed a limiting value on the pore size [13]. SANS has also been used to characterise a model of a biological membrane, supported in AAO membranes [14]. All these studies were restricted to AAO films marketed commercially as filters, with two different pore openings (20nm and 200 nm) based on a main pore diameter of 200nm.

We have now used SAXS to make a systematic study of AAO membranes with a range of different pore diameters. Our aim was to evaluate the extent to which SAXS can more fully characterise the structure of these materials on several different length scales: pore diameter, pore separation, the long-range regularity of pore separation, pore length and aspect ratio, pore continuity and variation of pore diameter along the length [15]. For membranes containing metal nanowires, important additional parameters are the proportion of pores containing metal, the regularity of distribution of full and empty pores, and the degree to which individual pores are filled with metal.

2. EXPERIMENTAL

Mesoporous alumina membranes were prepared by anodising electropolished high-purity aluminium foils in a polyprotic acid such as sulfuric or oxalic acid, using a lead plate cathode, followed by removal of the membrane from the Al backing. Details are described elsewhere [5,15]. Anodising voltages from 4 V to 60 V were used, giving membranes with pore diameters between 5 nm and 72 nm as confirmed by SEM measurements. **Fig. 1** shows a typical AFM image of a membrane prepared using a voltage of 40 V. Membrane thickness was controlled by varying the anodising time, and ranged between a few hundred nanometres and several hundred microns. The 40 V membranes discussed in this paper had a thickness of 35 microns. Cobalt nanowires were deposited within the porous membranes, before their removal from the Al backing, by electrochemical plating from an aqueous $CoSO_4$ solution using H_3BO_3 as a supporting electrolyte [6].

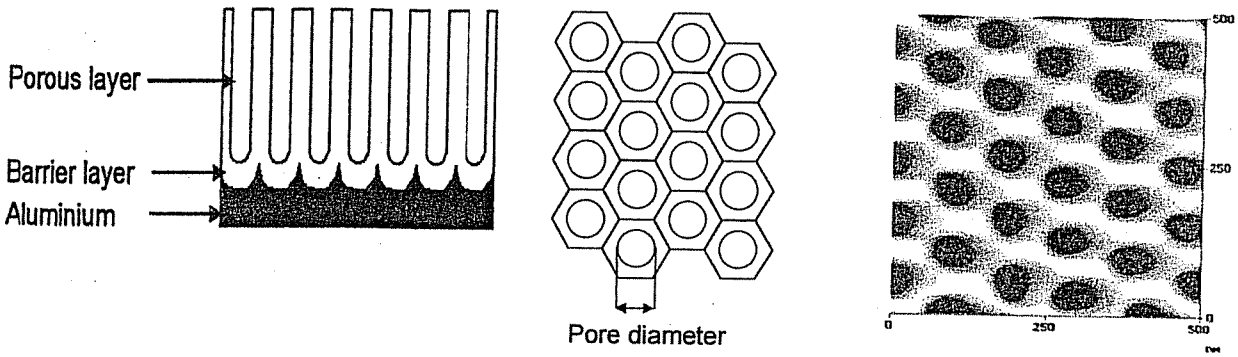

Fig 1 Structural features of the mesoporous alumina membranes: Schematic cross section (before removal of Al backing) and schematic top view, together with an atomic force microscope AFM (Voltage) image for a membrane produced by anodisation at 40 V.

The SAXS experiments were conducted on beamline ID01 at the ESRF (Grenoble, France) using an incident wavelength of 1.54Å. A three-circle sample mount enabled the membrane orientation to be precisely varied by remote control. The beam size of 3.0 mm x 0.2 mm provided 10^{12} photons/sec at the sample position. SAXS intensity profiles were measured with a 2D gas-filled wire detector, consisting of an active array 230 mm x 230 mm with resolution of $(179\ \mu m)^2$. The central area was masked by a 6 mm diameter beamstop. The detector was positioned 4.5 m from the sample, giving a range of scattering vector $k = (4\pi/\lambda)\sin(\theta/2)$ from 0.005 to 1.2 nm^{-1}. Extremely high forward scattering intensity was observed from the membrane samples, so an attenuator was used in the X-ray beam. Similar intensity enhancement when the orientation of the array of pores is parallel to the beam has also been observed in small-angle neutron scattering [14]. Counting times were typically 5 minutes. Background counts, recorded with an empty sample holder, were very low and there was no significant difference between background-subtracted and uncorrected datasets. Data analysis was carried out using the program FIT2D [16].

3. EMPTY MEMBRANES

Samples with the face of the membrane perpendicular to the incident X-ray beam (i.e. with pores parallel to the beam) gave ring patterns [15] as shown in **Fig. 2a** for the 40V membrane. Rotation of the sample position about two axes to optimise this pattern allowed the sample orientation to be defined as perpendicular to the beam to within better than 0.2°.

Rotation of the membranes about the vertical axis covered all possible orientations, as there is cylindrical symmetry around the beam axis.

When the membranes were rotated about a vertical axis, the SAXS patterns changed systematically through a complex sequence, developing an anisotropy that was dependent on the membrane orientation. For membranes edge-on to the incident X-ray beam, with pore axes effectively in a horizontal direction perpendicular to the beam, the anisotropy increased to the limiting case where the SAXS intensity was confined to a set of vertical spots (**Fig. 2b**). In this geometry the coherent scattering is restricted to the vertical direction if the cylinder axes are accurately parallel. **Fig. 2b** shows that deviations from the spot pattern are very small, proving that the pore axes in the AAO membranes are parallel to within ±0.2°.

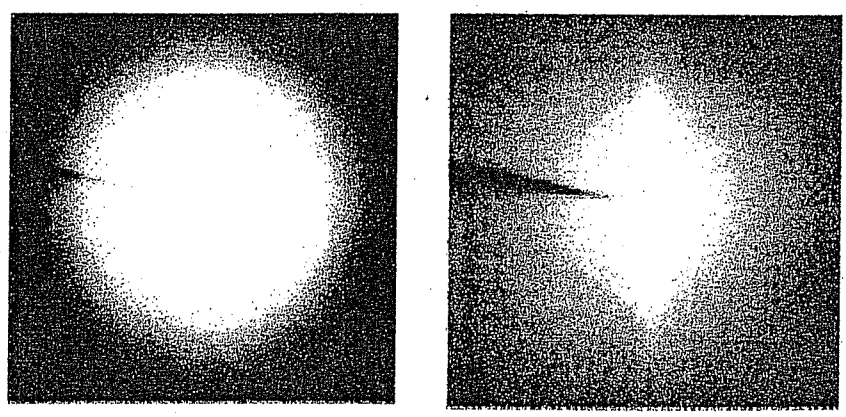

Fig. 2 SAXS patterns observed from 40 V alumina membrane.
(a, left) with the face of the membrane perpendicular to the incident X-ray beam
(b, right) with the membrane edge-on to the beam.

The SAXS intensity profile is a product of the cylinder form-factor for the individual pores and a two-dimensional structure factor for the disordered array of parallel channels. The general intensity profile for an assembly of parallel pores oriented at an angle to the incident beam is very complex, and no general analytic expression for the intensity distribution for any orientation of a defined cylinder array has yet been derived. Consequently, a full analytical interpretation of the data is not yet possible. Quantitative data can best conveniently be extracted by studying radial summations of the two-dimensional SAXS data, summing the intensity values around the ring [15].

Fig. 3 shows typical results for 20V, 40V and 60V membranes face-on to the beam. The intensity varies over five orders of magnitude and is presented as a log-log plot. Similar profiles were obtained from membranes edge-on to the beam, and from membranes of different thicknesses.

The general shape is similar for all three samples. A regular oscillatory pattern is clearly defined over four periods, covering a k-range of 0.02 to 0.5 nm^{-1}, but displaced to different k-values for each sample. These features arise from Bragg peaks in the structure factor from the two-dimensional hexagonal array of pores. The first peak position, k_0, is related to a spatial dimension, d, given by $d = 2\pi/k_0$ and corresponding to the mean separation of the pore axes. An increased membrane growth voltage gives a larger pore size and separation distance, so the first peak is displaced to lower k-values. The results, combined with those from membranes grown at other voltages, confirm the linear relationship between anodic growth voltage and pore separation, with a slope of 2.1 nm V^{-1}.

The Bragg peaks are broad, and do not give the full range of sharp peaks expected for a perfect hexagonal lattice. This shows that the AAO membranes have pore distributions that are more disordered than apparent from images of their surface structure (**Fig. 1**), which cover only a limited area. The variation in magnitude of the oscillations in the curves indicate that the 20 V membranes have the most regular arrangement of pore axes.

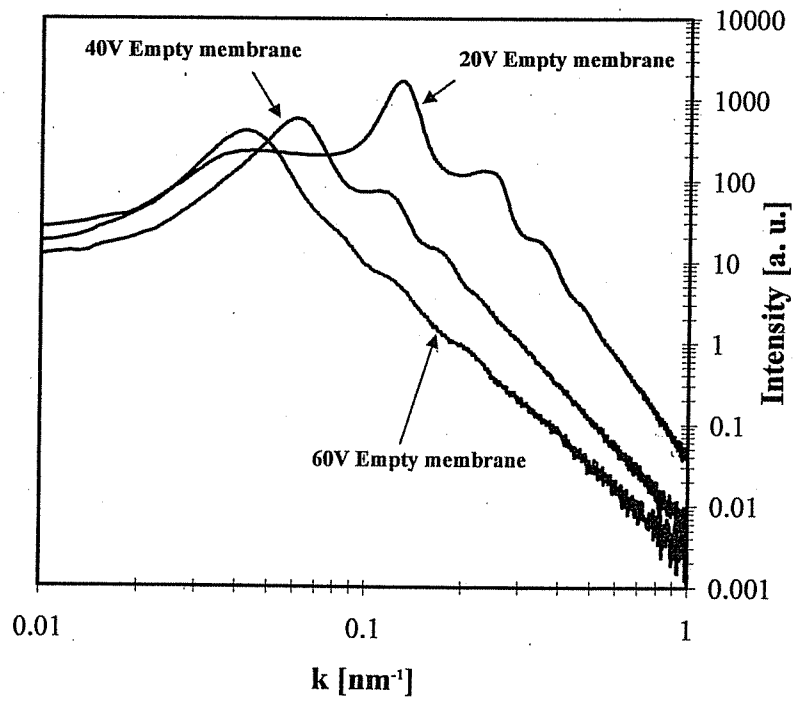

Fig 3. Experimental SAXS intensity profile (log-log plot) for mesoporous alumina membranes grown at 20 V, 40 V and 60 V. The membranes were face-on to the X-ray beam.

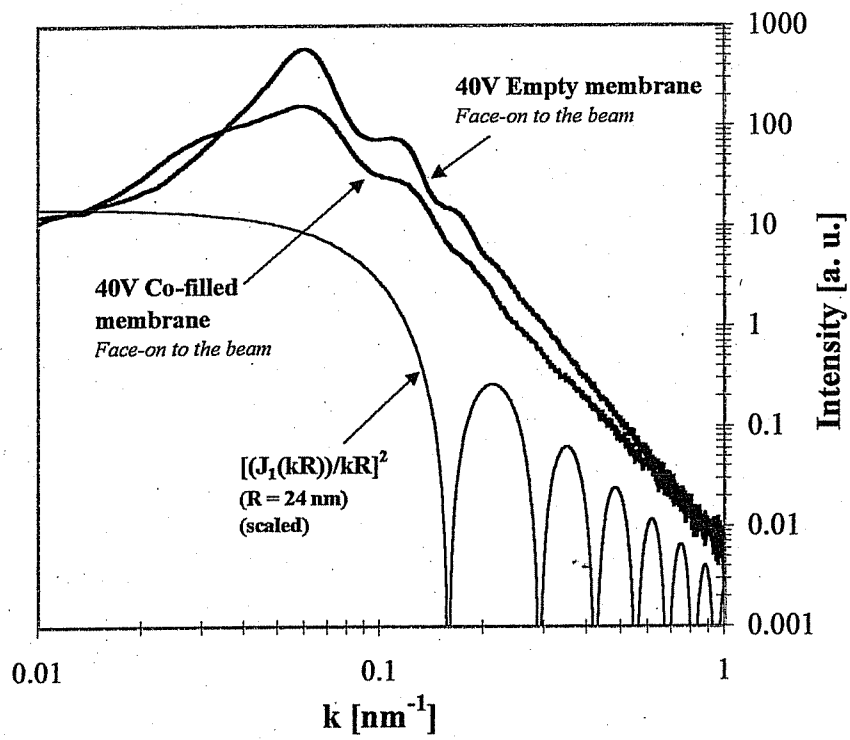

Fig. 4 SAXS intensity profile from a 40V cobalt-filled AAO membrane in the face-on position, compared with that from an empty 40V membrane. The Bessel function dependence of the cylinder form-factor with R = 24 nm, scaled for ease of comparison with the intensity curves, is also shown.

Clearly, the structure factor dominates the SAXS patterns. It is relevant to ask whether the cylinder form factor, depending on the pore radius, also plays a significant role in the scattering distribution. The calculated cylinder form factor is defined by a Bessel function [12,15,17] which has zeroes at specific k-values. As shown in **Fig 4,** the experimental profiles for 40 V membranes (pore diameter 48nm) do not display a clear link to this pattern. The predicted first minimum is close to the broad third-order structure factor peak. It is consequently impossible to derive a value for the pore radius directly from the results without a more detailed analytic treatment. This is disappointing, as the pore size is fundamentally important in the use of AAO membranes in filtration or as templates. Electron microscopy studies show that for the synthetic conditions employed, pore diameters above 12nm are linearly related to anode voltage (1.2 nm/V) and so are approximately half the mean pore separation [7,15].

The SAXS patterns at higher k-values display asymptotic linear slopes indicating a power law relation. For a sharp interface with a smooth geometry, the intensity is expected to follow a k^{-4} power law in this Porod region. The observed slope varies systematically with pore size, membrane orientation and thickness. In some cases, exponents more negative than 4 are observed. This may arise from either angulosity or a non-sharp interface, and is discussed in more detail elsewhere [15].

4. MEMBRANES FILLED WITH COBALT NANOWIRES

In SAXS, the amplitude function of the coherently-scattered monochromatic X-ray beam is proportional to the electron density distribution $\rho_e(\mathbf{r})$ integrated over the sample volume. In a two-phase porous medium such as the AAO membranes, the electron density is defined by two possible values, and we may write the spatial distribution as:

$\rho_e(\mathbf{r}) = \Delta\rho\, f(\mathbf{r})$ with $\Delta\rho = \rho_s - \rho_v$

where ρ_s and ρ_v are the electron densities for the solid matrix and the void volume respectively; $f(\mathbf{r})$ is a form-factor which is defined by the geometry of the pores. If the pores are empty, $\rho_v = 0$, but if they are filled with another material, ρ_v is finite and the magnitude of $\Delta\rho$ depends on the contrast between the two values of the electron density. If the pore contents have the same electron density as the host matrix, then $\Delta\rho = 0$, and the scattering intensity (proportional to the square of the amplitude function) will be zero. This technique is known as contrast matching. Any observed scattering will then give detailed information on the degree and regularity of pore-filling, and on inhomogeneities in the interface region, as voids in the filling medium convert the assembly to a three-phase system.

Table 1 shows electron density values ρ_e for porous solids (Al_2O_3, SiO_2), and some molecular liquids and metals relevant in various applications of AAO membranes. Several liquid halogenated hydrocarbons with ρ_e in the same range as SiO_2 have been used for contrast matching in SAXS studies of porous silicas [18]. However, Al_2O_3 has strong ionic bonding leading to a high density. Alumina membranes therefore have a higher electron density than SiO_2 and cannot be X-ray contrast matched with these molecular liquids, even allowing for the fact that AAO consists of poorly crystalline gamma-alumina rather than corundum. Conversely, the metals deposited as nanowires in AAO membranes [5,6] have ρ_e values too high to give a contrast match with the alumina host matrix.

Instead of attempting to contrast match, we chose cobalt as a pore-filling material. The contrast values $\Delta\rho$ for alumina/void and alumina/cobalt, from **Table 1**, are of opposite sign but close in magnitude. If the cobalt completely occupies the pore cavities, the intensity profile should therefore have the same shape as that for the empty membrane.

Structural studies (high energy X-ray diffraction and cobalt K-edge EXAFS) [6], together with NMR studies by others [19], have shown that cobalt nanowires within the pores of AAO membranes are a mixture of fcc and hcp structures. In bulk cobalt, the fcc phase is stable only at high temperatures. The hcp phase has the same lattice structure as bulk Co, but the orientation of the c-axis and the magnetic axis within the pores are important issues in understanding the unusual ferromagnetic properties of these nanoscale materials [6,20]. The regularity of pore filling is also of importance.

Table 1 Relative total electron density values ρ_e for several materials

Material	*Density (ρ_m) ($g\ cm^{-3}$)*	*Electron density (ρ_e) (10^3 electrons nm^{-3})*
Al_2O_3 (corundum)	3.96	1.17
Al_2O_3 (gamma)	3.5 – 3.9	1.03 – 1.15
SiO_2 (quartz)	2.64	0.79
SiO_2 (cristoballite)	2.32	0.70
CBr_4	3.42	0.91
$CHBr_3$	2.89	0.77
CH_2Br_2	2.49	0.67
H_2O	1.00	0.33
Fe	7.87	2.20
Co	8.80	2.45
Ag	10.50	2.75
Au	19.32	4.67
Sn	7.28	1.85

Fig. 4 illustrates the general features of the SAXS patterns obtained from AAO membranes containing cobalt nanowires. The intensity profile from a 40V cobalt-filled AAO membrane (pore diameter 48 nm) in the face-on position is compared with that from an empty 40V membrane. There is a much more substantial modification of the SAXS pattern than expected. The peaks from the cobalt-filled membrane are displaced to slightly higher k-values; the oscillatory amplitude is reduced; and there is an additional broad subsidiary peak at lower k-values ($k=0.033$ nm^{-1}).

This behaviour in the intensity patterns is unexpected. We have observed similar effects in cobalt-filled membranes with different pore sizes, and also in initial experiments on membranes with pores filled by other metals such as silver [21]. This suggests that the distribution of the metal in the pores does not correspond to the void volume of the empty pores, leading to increased disorder in the SAXS profile. Some nanowires may be discontinuous, or there may be some empty pores. More studies are needed to ensure that the electrochemical nanowire deposition process does not change the membrane mesostructure. Absorption effects, which are usually neglected in the SAXS formalism, may also be important for this geometry and an attenuation factor might be required in the theoretical treatment of the coherently-scattered waves. This also raises the interesting possibility of using anomalous scattering methods, such as ASAXS, near an absorption edge for the metallic substrate to study the behaviour in more detail.

5. CONCLUSIONS

Structural characterisation of AAO membranes by SAXS complements and extends direct-imaging methods such as electron microscopy, which view only the surface structure for a limited area of the sample. The ability to measure anisotropic X-ray scattering with a two-dimensional detector is particularly significant, allowing study of changes in the SAXS patterns caused by rotation of the membranes. The dominant characteristic in the intensity profile is the distribution of the 2D hexagonal pore array, and the results indicate that there is greater disorder than normally deduced from other techniques. Cobalt-filled membranes show significant changes in the SAXS profile, which can be attributed to incomplete filling of the pore volume and/or X-ray attenuation. The initial studies presented here have opened up a new range of possibilities for quantitative determination of pore characteristics in AAO membranes using synchrotron X-ray techniques.

ACKNOWLEDGEMENTS

For financial support we thank the EU TMR programme [22] contract number FMRX-CT98-0177. MK acknowledges a grant funded by Deutsche Forschungsgemeinschaft (DFG). The X-ray studies at the ESRF were supported by the EPSRC programme for work on international facilities.

REFERENCES

[1] J. W. Diggle, T. C. Downie & C. W. Goulding, Chem. Rev., 69 (1969) 365.
[2] J. P. O'Sullivan & G. C. Wood, Proc. Roy. Soc. Lond., A 317 (1970) 511.
[3] J. C. Hulteen & C. R. Martin, J. Mater. Chem., 7 (1997) 1075.
[4] T.-A. Hanaoka, A. Heilmann, M. Kröll, H.-P. Kormann, T. Sawitowski, G. Schmid, P. Jutzi, A. Klipp, U. Kreibig & R. Neuendorf, Appl. Organometal. Chem., 12 (1998) 367.

[5] R. E. Benfield, D. Grandjean, R. Pugin, T. Sawitowski, M. Kröll & G. Schmid, J. Phys. Chem. B, 105 (2001) 1960.
[6] R. E. Benfield, D. Grandjean, J. C. Dore, Z. Wu, T. Sawitowski, M. Kröll & G. Schmid, Eur. Phys. J. D, 16 (2001) 399.
[7] G. Hornyak, M. Kröll, R. Pugin, T. Sawitowski, G. Schmid, J.-O. Bovin, G. Karsson, H. Hofmeister & S. Hopfe, Chem. Eur. J., 3 (1997) 1951.
[8] T. Hanaoka, H-P. Kormann, M. Kröll, T. Sawitowski & G. Schmid, Eur. J. Inorg. Chem., (1998) 807.
[9] T. Kyotani, B. K. Pradhan & A. Tomita, Bull. Chem. Soc. Japan, 72 (1999) 1957.
[10] J. C. Dore, A. Burian, T. Kyotani and V. Honkimaki, in preparation; J. C. Dore, A. Burian, T. Kyotani & V. Honkimaki, ESRF Scientific Highlights (2001) 23.
[11] A. Heilmann, F. Altmann, D. Katzer, F. Müller, T. Sawitowski & G. Schmid, App. Surf. Sci., 144-145 (1999) 682.
[12] J. S. Rigden, J. C. Dore & A. N. North, Stud. Surf. Sci. Catal., 87 (1994) 263.
[13] L. Auvray, S. Kallus, G. Golemme, G. Nabias & J. D. F. Ramsay, Stud. Surf. Sci. Catal., 128 (2000) 459.
[14] D. Marchal, C. Bourdillon & B. Demé, Langmuir, 17 (2001) 8313.
[15] D. Grandjean, J. C. Dore, R. E. Benfield, M. Kröll, G. Schmid & D. Le Bolloc'h, submitted for publication.
[16] A. P. Hammersley, ESRF Internal Report ESRF97HA02T, "FIT2D: An Introduction and Overview", (1997).
[17] I. Livsey, J. Chem. Soc., Faraday Trans 2, 83 (1987) 1445.
[18] D. W. Hua, J. V. D'Souza, P. W. Schmidt & D. M. Smith, Stud. Surf. Sci. Catal., 87 (1994) 255.
[19] G.J. Strijkers, J.H.J. Dalderop, M.A.A. Broeksteeg, H.J.M. Swagten & W.J.M. de Jonge, J. Appl. Phys., 86 (1999) 5141.
[20] P. Paulus, F. Luis, M. Kröll, G. Schmid, & L. J. de Jongh, J. Magn. Magn. Mater., 224 (2001) 180.
[21] R. E. Benfield, D. Grandjean, J. C. Dore, M. Kröll & G. Schmid, work in progress.
[22] EU TMR project "CLUPOS". Homepage: www.clupos.lth.se